BRAIN
A JOURNAL OF NEUROLOGY

Spatio-temporal mapping cortical neuroplasticity in carpal tunnel syndrome

Rupali P. Dhond,[1] Emily Ruzich,[1] Thomas Witzel,[1] Yumi Maeda,[1,2] Cristina Malatesta,[3] Leslie R. Morse,[4] Joseph Audette,[5] Matti Hämäläinen,[1] Norman Kettner[2] and Vitaly Napadow[1,2]

1 Martinos Center for Biomedical Imaging, Department of Radiology, Massachusetts General Hospital, Harvard Medical School, Charlestown, MA 02129, USA
2 Department of Radiology, Logan College of Chiropractic, Chesterfield, MO 63017, USA
3 Department of Physical Medicine and Rehabilitation, Harvard Medical School, Spaulding Rehabilitation Hospital, Medford, MA 02155, USA
4 Department of Physical Medicine and Rehabilitation, Harvard Medical School, Spaulding Rehabilitation Hospital, Boston, MA 02114, USA
5 Department of Pain Medicine, Harvard Vanguard Medical Associates, Atrius Health, Boston, MA 02215, USA

Correspondence to: Rupali P. Dhond,
Martinos Center for Biomedical Imaging,
MGH-CNY, Building 149, 13th Street,
Room 2301,
Charlestown, MA 02129, USA,
E-mail: polly@nmr.mgh.harvard.edu

Neuroimaging data demonstrate that carpal tunnel syndrome, a peripheral neuropathy, is accompanied by maladaptive central neuroplasticity. To further investigate this phenomenon, we collected magnetoencephalography data from 12 patients with carpal tunnel syndrome and 12 healthy control subjects undergoing somatosensory stimulation of the median nerve-innervated Digits 2 and 3, as well as Digit 5, which is innervated by the ulnar nerve. Nerve conduction velocity and psychophysical data were acquired to determine whether standard clinical measures correlated with brain response. In subjects with carpal tunnel syndrome, but not healthy controls, sensory nerve conduction velocity for Digits 2 and 3 was slower than Digit 5. However, somatosensory M20 latencies for Digits 2 and 3 were significantly longer than those of Digit 5. The extent of the M20 delay for median nerve-innervated Digit 2 was positively correlated with decreasing nerve conduction velocity and increasing pain severity. Thus, slower peripheral nerve conduction in carpal tunnel syndrome corresponds to greater delays in the first somatosensory cortical response. Furthermore, spectral analysis demonstrated weaker post-stimulus beta event-related desynchronization and earlier and shorter event-related synchronization in subjects with carpal tunnel syndrome. The extent of the decreased event-related desynchronization for median nerve-innervated digits was positively correlated with paraesthesia severity. We propose that ongoing paraesthesias in median nerve-innervated digits render their corresponding sensorimotor cortical areas 'busy', thus reducing their capacity to process external stimulation. Finally, subjects with carpal tunnel syndrome demonstrated a smaller cortical source separation for Digits 2 and 3 compared with healthy controls. This supports our hypothesis that ongoing paraesthesias promote blurring of median nerve-innervated digit representations through Hebbian plasticity mechanisms. In summary, this study reveals significant correlation between the clinical severity of carpal tunnel syndrome and the latency of the early M20, as well as the strength of long latency beta oscillations. These temporal magnetoencephalography measures are novel markers of neuroplasticity in carpal tunnel syndrome and could be used to study central changes that may occur following clinical intervention.

Introduction

Carpal tunnel syndrome, a focal neuropathy, affects ~3.7% of the general public in the USA and occurs most often in females (OWH, 2009). In carpal tunnel syndrome, the median nerve, which innervates the first three digits of the hand and part of the fourth, becomes compressed within the carpal tunnel at the wrist (Katz and Simmons, 2002). This compression produces slowed, or in severe cases blocked, signal conduction as exemplified by decreased sensory and/or motor nerve conduction velocity. The most common symptoms of carpal tunnel syndrome include pain, paraesthesias (tingling, burning and itching), numbness and even weakness in the affected hand. Although the aetiology of carpal tunnel syndrome is much debated, both repetitive motion/strain (Silverstein *et al.*, 1987) and genetic predisposition (Hakim *et al.*, 2002) have been implicated. In 2003, the average number of missed work days because of carpal tunnel syndrome was 23, costing > $2 billion a year as reported by the U.S. Department of Labour (OWH, 2009).

Although it is a peripheral neuropathy, neuroimaging data suggest that the irregular afferent signalling occurring in carpal tunnel syndrome produces maladaptive central neuroplasticity. For example, spinal amplification of event-related potentials to ulnar nerve stimulation of the carpal tunnel syndrome affected hand is thought to represent unmasking of secondary inputs that are silent in the case of normal median nerve signalling (Tinazzi *et al.*, 1998). Cortical amplification of early evoked responses following stimulation of median nerve-innervated digits and altered S1 digit somatotopy has also been reported (Druschky *et al.*, 2000; Tecchio *et al.*, 2002). These general findings have recently been confirmed by functional MRI data (Napadow *et al.*, 2006).

However, altered somatotopy and amplification may not be the only evidence of modified central processing in carpal tunnel syndrome. In the present study, we hypothesized that delayed nerve conduction at peripheral sites should also be accompanied by delayed cortical response. Second, we hypothesized that in carpal tunnel syndrome, cortical rhythms may be altered because of ongoing symptoms of pain and paraesthesias. Although surgery is a definitive treatment for carpal tunnel syndrome, in rare cases, symptoms remain after carpal tunnel release (Katz *et al.*, 1998), suggesting that pain may have become centralized. Indeed, studies in central neuropathic pain populations demonstrate modification of sensorimotor rhythms following innocuous and noxious stimulation (Juottonen *et al.*, 2002; Kirveskari *et al.*, 2010). Thus, even though carpal tunnel syndrome is a peripheral neuropathy, neuroimaging its central correlates may provide insight to the stages of cortical response modification that lead to the centralization of pain.

To test these hypotheses, we used anatomically constrained magnetoencephalography (MEG) to map spatio-temporally differences in somatosensory brain response between carpal tunnel syndrome and healthy control subjects undergoing electrostimulation of median nerve-innervated Digits 2 and 3 and ulnar nerve-innervated Digit 5. Furthermore, we evaluated how spatio-temporal brain markers of carpal tunnel syndrome compared with well-known clinical metrics such as nerve conduction velocity and symptom ratings taken from the same subjects.

Materials and methods

Subject recruitment, neurophysiological and psychophysical evaluation

Data were collected from 12 patients with mild to moderate carpal tunnel syndrome (nine females, three males; mean age = 45.0 ± 8.3 years) and 12 healthy control subjects (four females, eight males; mean age = 46.1 ± 8.3 years). Most of the subjects with carpal tunnel syndrome were bilateral, and five had mild and seven had moderate forms of the syndrome. All subjects were recruited according to guidelines set by Partners Research Management and Massachusetts General Hospital.

To determine eligibility, subjects underwent clinical evaluation, which included screening by medical history, sensory and motor nerve conduction testing (Cadwell Sierra EMG/NCS Device), Tinel's Sign (Tinel, 2005) and Phalen's Manoeuvre (Phalen, 1966). All subjects completed the Edinburgh Handedness Questionnaire (Oldfield, 1971), and subjects with carpal tunnel syndrome were further evaluated using the Boston Carpal Tunnel Questionnaire (Levine *et al.*, 1993). Patients with carpal tunnel syndrome who reported pain and/or paraesthesias for > 3 months in the affected hand (specifically, in digits innervated by the median nerve) were enrolled. Patients were categorized as having mild, moderate or severe carpal tunnel syndrome (AAEM, 1993). Age and gender-matched healthy control subjects were also evaluated to ensure they did not suffer from carpal tunnel syndrome. Subject exclusion criteria included history of psychiatric/neurological disorder; head trauma; loss of consciousness; cardiovascular, respiratory or renal illness; wrist fracture with trauma to the median nerve; localized ulnar nerve entrapment or generalized peripheral neuropathy not attributable to carpal tunnel syndrome; bleeding disorders and use of anticoagulants, opioids or psychotropic medications. Contraindications for MRI/MEG scanning were pregnancy, pacemakers and metallic implants. Written informed consent was obtained for all subjects before enrolment and each imaging scan. All subjects were compensated for participation in each imaging session.

Furthermore, psychomotor performance and tactile discrimination ability were assessed using pinch grip testing (BTE Work Simulator) and vibrotactile biobehavioural testing, respectively. Pinch grip was measured using an in-house-constructed feedback system. In addition to calculating maximum voluntary contraction using pinch grip, subjects were instructed to pinch and release the grip test apparatus as quickly as possible between two visually guided limits: 2% maximum voluntary contraction and 25% maximum voluntary contraction. This was done to evaluate fine motor control, which is disrupted in carpal tunnel syndrome (Radwin *et al.*, 2004). Tactile discrimination was estimated with biobehavioural testing using a voice coil actuator device (model CM-4, Cortical Metrics; Zhang *et al.*, 2011). Subjects received vibrotactile stimulation (25 Hz, 500 ms) over four digits (Digits 2–5). Subjects did not know which digit was being stimulated and were asked to respond with the opposite hand when they could identify the stimulated finger.

Experimental stimulation

To evaluate brain responses to stimulation of affected areas, subjects underwent low-frequency electro-stimulation at Digit 2 (index finger),
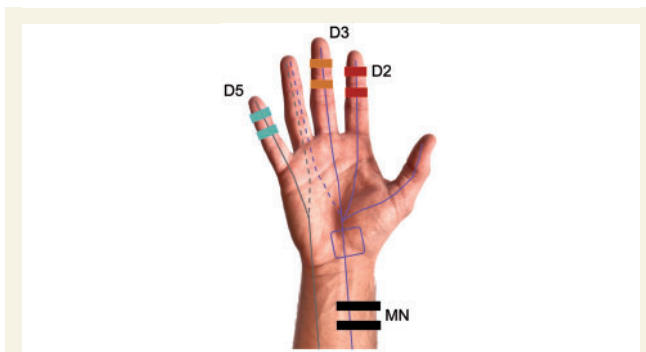
Figure 1 Hand stimulation sites. The median nerve (MN) innervates the first three digits (purple lines) and part of the fourth, whereas the ulnar nerve innervates the fifth digit and part of the fourth (grey lines). In carpal tunnel syndrome, the median nerve becomes entrapped within the carpal tunnel (purple box). The ulnar nerve is not affected in carpal tunnel syndrome. Subjects were stimulated at four locations: the index Digit 2 (D2, red), middle Digit 3 (D3, orange), pinky Digit 5 (D5, blue) fingers and the median nerve (black) at a location proximal to the entrapment site.

Digit 3 (middle finger) and Digit 5 (pinky) and sub-motor stimulation of the median nerve proximal to the entrapment site (Fig. 1). To avoid potential confounds related to cortical representation size of the dominant versus non-dominant hand, all stimulation was given on the dominant (for healthy controls) or most affected (for carpal tunnel syndrome) hand. Specifically, 22 of 24 subjects were right handed. All subjects were stimulated on their dominant hand except for two subjects with carpal tunnel syndrome. The first of these had undergone surgery for carpal tunnel syndrome on their dominant hand, whereas the second subject was bilaterally affected but had more severe symptoms in the non-dominant hand.

Electrical current (0.2-ms pulse, interstimulus interval = 1.3 s) was provided by a GRASS stimulator (S88 Dual Output Square Pulse Stimulator, Grass Telefactor) and delivered through disposable ring electrodes (Viasys Healthcare Inc.) placed on the middle and distal phalanges of the digit. Stimulus intensity was set at roughly 2.5 mA above individual detection level. All subjects confirmed the stimulation level as being 'strong but not painful'. There were no significant differences in the stimulation intensities used for digit stimulation in subjects with carpal tunnel syndrome (5.94 ± 0.4 mA) and healthy controls (5.46 ± 0.2 mA) subjects. A plastic arm brace was used to prevent excessive movement or clenching of the hand or fingers during stimulation. Up to 200 trials were collected for each stimulated site.

Magnetoencephalography data collection

MEG signals were recorded with a 306-channel Vectorview MEG system (Elekta Neuromag Oy). Data were collected in the supine position to minimize movement and slouching that often occur during seated recordings. The head position with respect to the MEG sensory array was determined with the help of head position indicator coils. Locations on the subject's scalp surface and the head position indicator coils were digitized using a Polhemus FastTrak digitizer to allow for accurate alignment of the MEG and MRI coordinate systems. The

acquisition bandwidth was 0–400 Hz with a 1500 samples/s digitization rate. The subject's ECG and electrooculogram were recorded simultaneously to control for and if necessary remove influence from physiological noise sources such as heart beat, eye blinks and eye saccading. The raw data were further processed using the signal space separation method (MaxFilter, Elekta Neuromag Oy) to reduce the contribution of magnetic fields originating from outside the subject's head, including the stimulation artefact.

Structural magnetic resonance image data collection

Individual anatomical MRI data were collected for creation of boundary element models, to constrain the MEG source estimates to the cortex and to visualize the results in the cortical surface anatomy. Subjects were scanned in a Siemens Trio 3.0 T MRI equipped with a 32-channel head coil (Siemens Medical). MP-RAGE images were acquired (resolution = 256×256 matrix, field of view = 256 mm, 176 slices, 1.0-mm slice thickness, echo time = 1.64 ms, repetition time = 2530 ms, inversion time = 1200 ms, flip angle = $7°$, spatial resolution = $1 \times 1 \times 1$ mm^3).

Distributed source estimates

Sources underlying the MEG signals were inferred using the minimum norm estimate (Hamalainen and Ilmoniemi, 1984). Anatomical MRI information was used to constrain the source locations to the cortical mantle. The currents producing the MEG signals were assumed to be approximately orthogonal to the cortical surface (Lin et al., 2006). The cortical surface geometry was generated with FreeSurfer software (Dale et al., 1999; Fischl et al., 1999a) using each subject's individual MRI (reconstructed from high resolution MP-RAGE images). For purposes of intersubject averaging, the reconstructed surface for each subject was morphed onto an average spherical representation, optimally aligning sulcal and gyral features across subjects while minimizing metric distortions and shear (Fischl et al., 1999b), and MEG response amplitude was mapped onto an average sulcal–gyral pattern. For the MEG forward calculation, we used the boundary element method, which assumes the head is composed of arbitrarily shaped compartments with constant electrical conductivity. We used in-house-developed software for extracting the surfaces separating the relevant compartments (scalp, skull and brain) from anatomical MRI data. The boundary element method was then used for calculating the signal expected at each MEG sensor, for each dipole location (deMunck, 1992; Oostendorp and Van Oosterom, 1992). To estimate the time courses of cortical response, we used the noise-normalized anatomically constrained linear estimation approach described by Dale et al. (2000). This approach is similar to the generalized least squares or weighted minimum norm solution (Hamalainen and Ilmoniemi, 1984), except that the modelled sources were constrained to lie in the cortical surface (Dale and Sereno, 1993), and the estimate was normalized for noise sensitivity such that source signal-to-noise ratio rather than current dipole moment was mapped (Dale et al., 2000). The noise normalization also has the effect of greatly reducing the variation in the point spread function between locations (Liu et al., 1998). This approach provides statistical parametric maps of cortical response, similar to the statistical maps typically generated using functional MRI or PET data, but with a millisecond temporal resolution. These methods have been used previously, e.g. in MEG studies of language and memory (Dale and Halgren, 2001; Dhond et al., 2001; Halgren et al., 2002; Marinkovic, 2004).

Comparative S1 response dynamics and digit somatotopy

To localize S1 Digits 2, 3 and 5 sources, a region of interest encompassing the 'Ω'-shaped passage along the contralateral central sulcus (roughly Brodmann areas 3, 1 and 2) was made for each subject. The somatosensory M20 is believed to be the first afferent cortical response, and its location is thought to indicate Brodmann area 3b (Wikstrom *et al.*, 1996; Mauguiere *et al.*, 1997*a*, *b*). For each finger, we extracted all source waveforms within this region of interest representing the hand S1 area, and in each subject, we took the location with the largest M20 response as the site of the earliest cortical response to the stimulus.

Digit separation distances were mapped for each subject using their reconstructed cortical surfaces. The distance calculations represent the shortest path along the cortical surface mesh between the Digit 2–Digit 3–Digit 5 sources (nodes). This was done using the FreeSurfer implementation of Dijkstra's shortest path algorithm (http://surfernmr.mgh.harvard.edu/). Significant differences were determined using two-sample Mann–Whitney U-tests ($P < 0.01$).

To determine whether there were differences in initial S1 response latencies, M20 peak latencies were compared for Digits 2 and 3 versus Digit 5 in both carpal tunnel syndrome and healthy control subjects using non-parametric Wilcoxon matched pairs tests. Comparisons were also made for Digit 2/Digit 3 between healthy control and carpal tunnel syndrome groups using non-parametric Mann–Whitney U-tests.

Spectral analysis

A time–frequency representation of the S1 source waveforms was computed to investigate induced activity during digit stimulation. Induced activity describes a change in the ongoing or endogenous oscillatory activity of the brain; this activity is not phase locked to the stimulus and cannot be seen with evoked spectral analyses. We used a continuous wavelet transform with complex Morlet wavelets (Goupillaud *et al.*, 1984). Continuous raw waveforms were wavelet transformed before separation into trials. This was done to prevent edge artefact contamination in the lower frequency spectrum. An average evoked time–frequency representation was calculated and subtracted from each individual trial before averaging for creation of the induced time–frequency representations. Relative change from the baseline mean as a function of time was calculated for each frequency individually to determine the level of event-related desynchronization and event-related synchronization (Graimann *et al.*, 2002). Other methods that could be used include functional source separation (Porcaro *et al.*, 2009).

Results

Psychophysical and neurophysiological outcomes

During patient recruitment, sensory and motor nerve conduction velocities were assessed to confirm carpal tunnel syndrome. The average median nerve peripheral sensory velocity (between digit and wrist) was slower for Digits 2 and 3 than for ulnar nerve-innervated Digit 5 (Table 1). Thus, afferent signalling in median nerve-innervated digits was slower. In contrast, healthy control subjects had roughly equal velocities for Digits 2, 3 and 5.

Table 1 Nerve conduction, tactile discrimination, motor performance and psychophysical rating values

Clinical Measurement	Carpal tunnel syndrome	Healthy control
Sensory nerve conduction velocity (m/s)		
Digit 2**	33.84 ± 4.4	55.95 ± 1.6
Digit 3**	32.64 ± 4.1	52.22 ± 1.8
Digit 5	52.34 ± 5.3	53.78 ± 1.6
Motor nerve peak latency (ms)		
Median**	5.43 ± 0.5	3.24 ± 0.1
Ulnar	2.79 ± 0.1	2.99 ± 0.1
Tactile discrimination		
Digit 2 response time (ms)*	533.50 ± 29.9	436.07 ± 45.6
Digit 3 response time (ms)	515.09 ± 36.8	433.86 ± 51.7
Digit 5 response time (ms)	524.82 ± 42.7	436.50 ± 48.2
Digit 2 response accuracy (% correct)	94.0 ± 4.0	100
Digit 3 response accuracy (% correct)*	92.0 ± 4.0	100
Digit 5 response accuracy (% correct)	93.0 ± 5.0	100
Pinch grip		
Maximum contraction (N)*	62.71 ± 5.2	80.73 ± 5.9
Pinch rate (s⁻¹)*	3.15 ± 0.3	4.2 ± 0.5
Overshoot (N)	0.24 ± 0.04	0.19 ± 0.03
Undershoot (N)	−0.06 ± 0.01	−0.08 ± 0.05
Boston Carpal Tunnel Questionnaire		
Pain ratings (1–5 scale)	2.73 ± 0.22	
Paraesthesia ratings (1–5 scale)	3.10 ± 0.24	

Group mean ± standard error values for clinical data. Significant differences between groups denoted by **$P < 0.01$ and *$P < 0.05$.

Median motor nerve peak latency in subjects with carpal tunnel syndrome was significantly longer than in healthy controls. No significant difference was seen between groups for ulnar motor nerve peak latency. Tactile discrimination testing demonstrated that subjects with carpal tunnel syndrome were slower to determine the stimulated finger and had a higher error rate when tested on the affected median nerve-innervated digits (Digits 2 and 3, respectively). Evaluation of fine motor performance with pinch grip testing demonstrated that subjects with carpal tunnel syndrome had both weaker maximum voluntary contraction and a slower rate of contraction than healthy controls. Assessment of symptom ratings using the Boston Carpal Tunnel Questionnaire (1–5 scale) showed that on average patients experienced stronger symptoms of paraesthesias than pain. Furthermore, evaluation of pain/paraesthesia ratios showed that in 8 of 12 subjects paraesthesias were the dominant symptom (0.80 ± 0.09).

Cortical responses to digit stimulation

To map the spatio-temporal dynamics of cortical response to finger stimulation, grand averages of digit stimulation trials (Digits 2, 3 and 5) were created (Fig. 2). In healthy control subjects, activity was clearly present in left (contralateral) S1 by ~26 ms post-stimulus but not in subjects with carpal tunnel
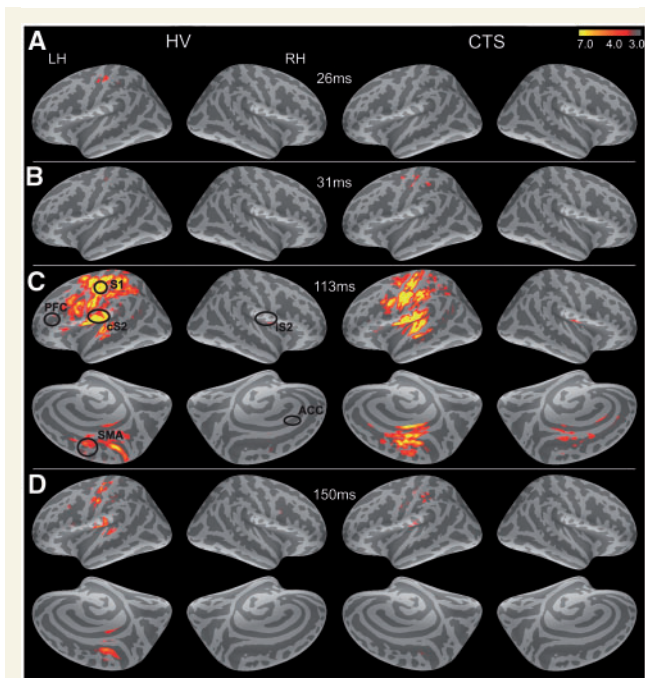
Figure 2 Grand average responses to digit stimulation. Stimulation of median and ulnar nerve-innervated digits evoked bilateral brain response with a characteristic temporal pattern. Responses are shown here on the average inflated surface (dark grey are sulci and light grey are gyri). (**A**) In healthy controls (HV), response first peaked in contralateral S1 cortex ~26 ms. (**B**) Initial S1 response appeared slightly later in subjects with carpal tunnel syndrome at ~31 ms post-stimulus. (**C**) By 113 ms post-stimulus, contralateral S2, ipsilateral S2 (iS2) and medial cortex including supplementary motor areas (SMAs) were active in both subject groups. In carpal tunnel syndrome, some response also localized within anterior cingulate areas (circle). (**D**) By 150 ms post-stimulus, all evoked responses had dissipated in both subject groups. PFC = prefrontal cortex.

syndrome until slightly later at ~31 ms (Fig. 2A and B). In both subject groups, response then spread to contralateral S2 by ~90 ms. By ~113 ms, response also occurred within ipsilateral (right) S2 regions and was present within contralateral supplementary motor area and cingulate cortex (Fig. 2C). MEG source localization to medial cortical areas during somatosensory stimulation has been noted previously (Forss et al., 1996). Response decreased in all areas by ~150 ms (Fig. 2D).

Differences in S1 and contralateral S2 evoked responses for carpal tunnel syndrome and healthy subjects

To determine how the timing of cortical responses was affected in carpal tunnel syndrome, we evaluated S1 source waveforms for each digit separately. Both healthy control subjects and patients with carpal tunnel syndrome demonstrated clear M20 and M30 responses followed by peaks at ~60 ms and 100–120 ms as shown in Fig. 3A. For each subject, individual M20 latencies for all digits

were compared. In subjects with carpal tunnel syndrome, the earliest Digit 2 (27.08 ± 1.3 ms) and Digit 3 (27.10 ± 2.4 ms) responses were longer than those for Digit 5 (24.20 ± 2.1 ms; Wilcoxon matched pairs tests: Digit 2 versus Digit 5, $P < 0.002$; Digit 3 versus Digit 5, $P < 0.008$). However, healthy control subjects did not have any significant differences in M20 latency between fingers, with an average response of 24.91 ± 3.1 ms for Digit 2, 24.00 ± 4.2 ms for Digit 3 and 24.83 ± 3.5 for Digit 5 (Fig. 3B). Although carpal tunnel syndrome latencies for Digits 2 and 3 were on average longer than those of healthy controls, these distributions were not significantly different (two-sample Mann–Whitney U-tests, $P > 0.05$).

In subjects with carpal tunnel syndrome, initial S1 response magnitude was slightly greater, but not significantly so, for Digit 2 compared with Digit 5. Digit 3 magnitude was significantly larger than that of Digit 5 at ~70–80 ms post-stimulus (two-tailed paired t-test, $P < 0.005$). No significant differences were present between digits in healthy controls or in the magnitude of S1 response between healthy control and carpal tunnel syndrome groups. To assess potential 'amplification' of early responses in carpal tunnel syndrome, M30/M20 ratios were calculated and compared for each digit. This ratio was significantly larger for Digit 2 (1.70 ± 0.4) compared with Digit 5 (0.79 ± 0.3) in paired t-tests ($P < 0.04$) but not for Digit 3 (1.57 ± 0.5) versus Digit 5. For healthy control subjects, there were no significant differences between Digit 2 (1.00 ± 0.3), Digit 3 (1.08 ± 0.4) and Digit 5 (1.49 ± 0.7).

In healthy control subjects, the magnitude of the Digit 2 contralateral S2 response (Fig. 3C) was larger than that of Digit 3 at ~55–125 ms (two-tailed paired t-test, $P < 0.005$). This was also the case in subjects with carpal tunnel syndrome, but it occurred later at ~75–110 ms. Additionally, in carpal tunnel syndrome, Digit 5 response was greater than Digit 3 and also Digit 2 at ~75–125 ms and 205–220 ms, respectively (two-tailed paired t-test, $P < 0.005$).

Dynamics of S1 alpha and beta oscillations

To assess differences in S1 source oscillatory dynamics between healthy controls and carpal tunnel syndrome subjects, average time–frequency representations of the per cent change from baseline for induced response were made. Time–frequency representations for median nerve-innervated (Digits 2 and 3) and ulnar nerve-innervated (Digit 5) digits are shown in Fig. 4A. Digit stimulation in healthy control and carpal tunnel syndrome subjects produced event-related desynchronization in the alpha band (α, 7–14 Hz) at ~100–500 ms post-stimulus. This was accompanied by beta band (β, 15–28 Hz) event-related desynchronization at ~100–350 ms post-stimulus and followed by beta event-related synchronization at ~400–750 ms. Although 11 of 12 subjects in each group demonstrated clear alpha and beta event-related desynchronization, only 8 of 12 subjects in each group demonstrated clear beta rebounds.

Comparisons were made between healthy control and carpal tunnel syndrome groups for alpha and beta bands. This was
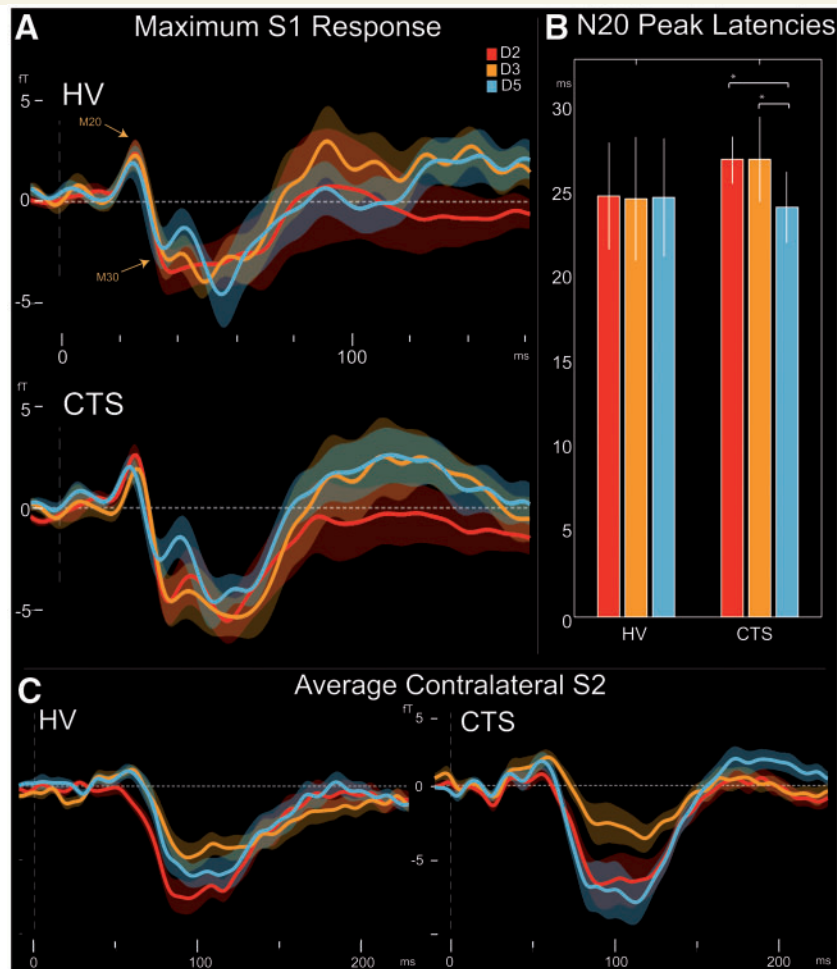
Figure 3 Evoked responses in healthy controls and carpal tunnel syndrome. (**A**) Healthy controls (HV) and subjects with carpal tunnel syndrome demonstrated M20 and M30 S1 peaks. Longer latency peaks at ~60 and ~100 ms were also present. Significantly larger M30/M20 ratio was also present for Digit 3 versus Digit 5 (paired tests, $P < 0.04$) in carpal tunnel syndrome. (**B**) Healthy controls showed no significant difference in M20 latency between median and ulnar nerve-innervated digits. However, in carpal tunnel syndrome, Digits 2 and 3 responses were slightly longer than those of Digit 5 (*$P < 0.002$, **$P < 0.008$). Thus, delayed signal transmission at the periphery leads to delayed onset of central responses at the level of S1. (**C**) For contralateral S2, Digit 2 response was larger than Digit 3 in healthy controls at ~55–125 ms and in carpal tunnel syndrome at ~75–110 ms ($P < 0.005$). Additionally, in carpal tunnel syndrome, Digit 5 response was greater than that of Digit 3 and also Digit 2 at ~75–125 ms and ~205–220 ms, respectively ($P < 0.005$). No significant differences were found between groups. Thus, evoked S2 response is not likely to be a consistent marker for median nerve abnormality in carpal tunnel syndrome.

done as a paired test of the absolute values for each time point between the 0–900 ms post-stimulus time window. On average, digit stimulation in the healthy control group produced greater alpha and beta event-related desynchronization than in the carpal tunnel syndrome group. However, differences were only significant for beta event-related desynchronization in median nerve-innervated digits at ~200–350 ms ($P < 0.005$, Mann–Whitney U-test; shown as grey box in Fig. 4B). Furthermore, onset timing for beta event-related synchronization was shorter ($P < 0.02$, Mann–Whitney U-test) in the carpal tunnel syndrome (369.83 ± 33.77 ms) than in the healthy control (472.64 ± 21.21 ms) groups.

Altered digit somatotopy in carpal tunnel syndrome

To investigate potential differences in cortical somatotopy between healthy controls and subjects with carpal tunnel syndrome, the distance between digit S1 sources was mapped for each subject. This was done using cortical surface reconstructions created from each subject's individual MRI. For both healthy controls and subjects with carpal tunnel syndrome, digit sources lay within the contralateral central sulcus roughly following the described somatotopic distribution of the hand (Penfield and Rasmussen, 1955). The average location of each digit was
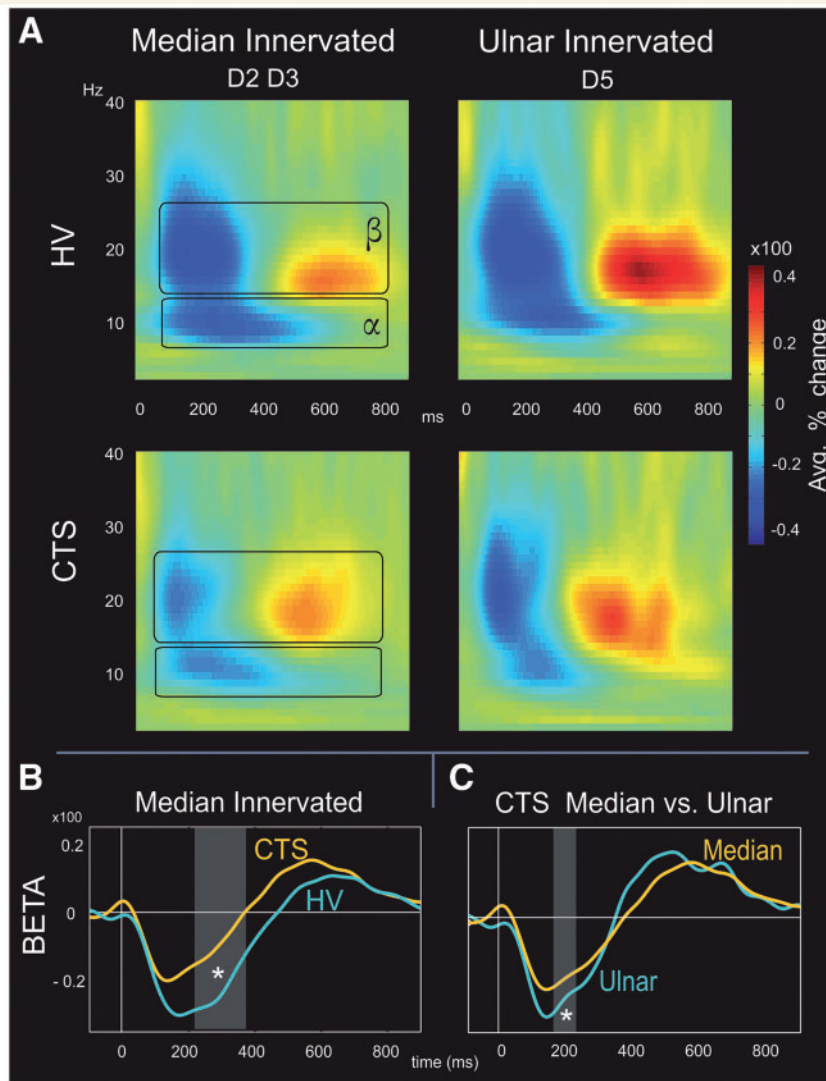
Figure 4 Oscillatory response to digit stimulation in healthy control and carpal tunnel syndrome. (**A**) In both subject groups, digit stimulation evoked alpha (7–14 Hz) and beta (15–28 Hz) event-related desynchronization from ~100–500 ms and ~100–350 ms, respectively (blue areas). This was followed by beta event-related synchronization (red areas) at ~400–750 ms. (**B**) On average, subjects with carpal tunnel syndrome demonstrated less alpha and beta event-related desynchronization than healthy controls. However, differences between groups were only significant in the beta band for median nerve-innervated digits between groups at ~200–350 ms (asterisk, grey rectangle). (**C**) Comparison of median and ulnar digits within each group showed that within carpal tunnel syndrome, greater event-related desynchronization was present for ulnar versus median nerve-innervated digits. This was not the case for healthy controls, suggesting that the extent of event-related desynchronization may be indicative of altered endogenous cortical processing in carpal tunnel syndrome.

determined by morphing individual surfaces and is shown in Fig. 5A. In both subject groups, Digit 2 sources localized most laterally followed by Digit 3 and finally by Digit 5 most medially.

In healthy control subjects, the Digit 2–Digit 3 separation distance (10.69 ± 1.1 mm) was significantly larger ($P < 0.05$, two-sample Mann–Whitney U-test) than that in subjects with (6.40 ± 0.67 mm). Although digit separation distances were shorter in subjects with carpal tunnel syndrome, there were no significant differences in the distributions between healthy control and carpal tunnel syndrome groups for Digit 3–Digit 5 distances (7.18 ± 0.72 mm versus 10.32 ± 1.38 mm) nor Digit

2–Digit 5 distances (14.47 ± 1.23 mm versus 11.13 ± 0.87 mm) (Fig. 5B).

Correlation of magnetoencephalography data with clinical metrics

To determine whether altered timing of brain responses was related to objective and subjective clinical assessment measures, we tested for correlations between S1 M20 peak latency and nerve conduction velocity as well as psychophysical ratings
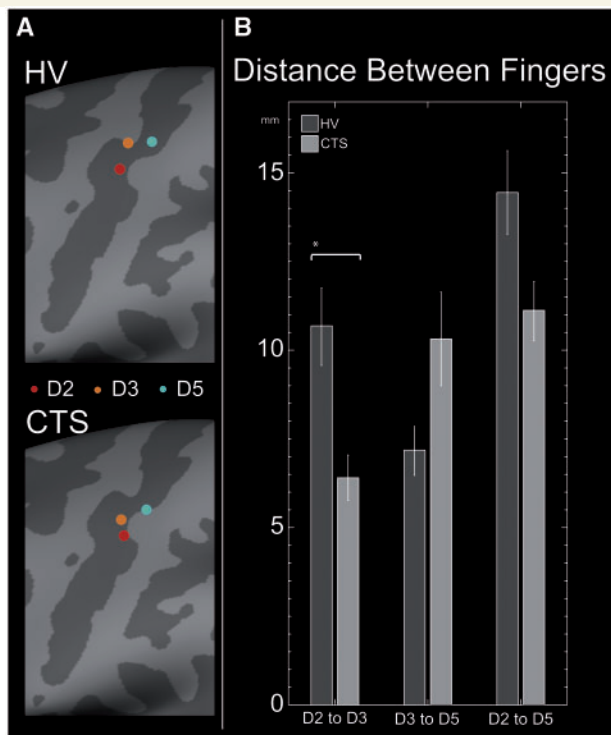
Figure 5 S1 digit somatotopy. (**A**) In both healthy controls (HV) and subjects with carpal tunnel syndrome (CTS), digit sources lay within the contralateral central sulcus. Here, average digit positions Digit 2 (red dot), Digit 3 (orange) and Digit 5 (blue) for each group are shown on the average inflated cortical surface. Specifically, dark grey represents sulci, whereas light grey represents gyri. In both subject groups, digit locations roughly followed the expected somatotopic distribution with index, middle and pinky digits mapping in a lateral to medial order. (**B**) All digit separation distances were shorter in carpal tunnel syndrome, but only the Digit 2–Digit 3 distances were significantly different in non-parametric tests (*$P < 0.05$, Mann–Whitney U-test).

(Boston Carpal Tunnel Questionnaire scores). Specifically, the extent of the difference between median nerve-innervated digits and ulnar nerve-innervated Digit 5 was calculated for each individual. Correlations were assessed using Spearman's *r*-test. We found that the M20 latency increase for median nerve-innervated Digit 2 (index minus pinky Digit 5) was negatively correlated ($r = -.75$, $P < 0.01$) with sensory nerve conduction velocity (Fig. 6A). Thus, greater delays in the timing of the first cortical response occur with decreasing sensory nerve velocity. Additionally, the M20 delay was positively correlated with increasing pain and overall symptom severity as determined by the Boston Carpal Tunnel Questionnaire.

Post-stimulus beta event-related desynchronization differences between median versus ulnar nerve-innervated digits were positively correlated with increasing intensity of paraesthesias (Fig. 6B). Changes in beta event-related desynchronization were not correlated with nerve conduction velocity. Thus, long latency modification in brain responses may represent more complex signalling alterations within the cortex.

Discussion

In this study, we used MEG to investigate how the timing of cortical-evoked responses and that of induced oscillatory activity are modified in carpal tunnel syndrome, a commonly experienced focal peripheral neuropathy.

S1-evoked response is altered in carpal tunnel syndrome

Cortical M20 is delayed in carpal tunnel syndrome

Subjects with carpal tunnel syndrome demonstrated a significant delay in S1 M20 latency for median nerve-innervated digits
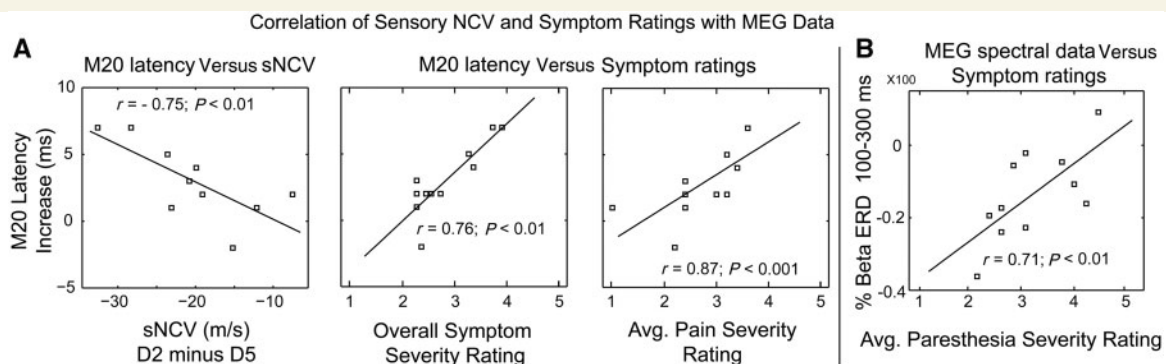

Figure 6 Correlation of MEG data with clinical neurophysiological assessment values. (**A**) The M20 latency increase for median nerve-innervated Digit 2 (D2) was negatively correlated with the decreased sensory nerve conduction velocity (NCV). Specifically, the greater the latency delay for the Digit 2 M20, the greater the decrease in Digit 2 sensory nerve velocity. Furthermore, changes in MEG data were positively correlated with symptom ratings on the Boston Carpal Tunnel Questionnaire. Thus, as M20 latency increased, so did overall symptom ratings and the severity of pain. (**B**) Post-stimulus beta event-related desynchronization differences between median versus ulnar nerve-innervated digits were positively correlated with increasing intensity of paraesthesias. Changes in beta event-related desynchronization were not correlated with nerve conduction velocity. Thus, long latency modification in brain responses may represent more complex signalling alterations within the cortex itself.

(Fig. 2A and B). In general, innocuous tactile information from peripheral body sites travels rapidly through the dorsal column–medial lemniscal pathway to the ventral posterolateral nucleus of the thalamus, which then projects to cortex. The M20 is thought to be the first cortical response to somatosensory stimulation, reflecting excitatory postsynaptic potentials resulting from activation of the basal dendrites of pyramidal cells by thalamo-cortical axons (Tiihonen et al., 1989; Wikstrom et al., 1996). We found that decreasing peripheral sensory nerve conduction velocity is significantly correlated with increasing delay at central sites, visible in the timing of the MEG M20. These data are the first to empirically demonstrate altered timing of the M20 in subjects with carpal tunnel syndrome.

Evoked response magnitude in carpal tunnel syndrome

Previous research has cited differences in spinal- and cortical-evoked response magnitudes as evidence of neuroplasticity in carpal tunnel syndrome (Tinazzi et al., 1998; Tecchio et al., 2002). Here, subjects with carpal tunnel syndrome demonstrated a significantly larger M30/M20 ratio for stimulation of median nerve-innervated Digit 2 compared with ulnar nerve-innervated Digit 5. However, evoked response was on average larger for Digits 2 and 3 versus Digit 5 stimulation at all latencies $>25\,ms$.

Animal research using induced deafferentation demonstrates that short-term neuroplasticity may occur via local 'disinhibition' and encroachment of neighbouring non-deafferented areas (Merzenich et al., 1983b; Calford and Tweedale, 1991). In relation to carpal tunnel syndrome, compression of the median nerve may produce local ischaemia (Seiler et al., 1989) followed by axonal damage and reduced regular afferent input from the affected digits. This altered signalling may release cortical pyramidal cells from normal inhibition by gamma-aminobutyric acidergic (GABAergic) interneurons (e.g. disinhibition). Thus, pre-existing excitatory thalamo-cortical and cortico-cortical synapses on the apical dendrites of cortical (i.e. layer 5) pyramidal cells now become 'unmasked' leaving these cells susceptible to over-excitation by the accumulation of previously subthreshold inputs (for a review of GABAergic cortical mechanisms see Mendez and Bacci, 2011). Although disinhibition has been used to explain the presence of larger event-related potentials for Digit 5 (versus median nerve) digit stimulation (Tinazzi et al., 1998), in the current data response, magnitude was larger for median nerve-innervated digit stimulation.

Furthermore, in the current data, the M30/M20 ratio was significantly larger for Digit 2 versus Digit 5 in subjects with carpal tunnel syndrome but for Digit 3 versus Digit 5 in subjects with carpal tunnel syndrome (within subject paired tests). As suggested by Tecchio et al. (2002), a larger M30/M20 ratio for median nerve-innervated digits may represent underlying 'cortical amplification', which in carpal tunnel syndrome would serve as a protective mechanism to counteract afferent signal attenuation. In general, neural amplification is thought to involve recurrent connectivity supporting positive feedback within excitatory cell populations; this prevents response decay and allows neurons to fire in the absence of input (Seung, 1996). However, the present group of subjects with carpal tunnel syndrome also demonstrated decreased S1 Digit 2–Digit 3 separation distance, i.e.

blurred median nerve-innervated digit representations. Thus, another interpretation is that larger Digit 2 M30 response represents co-activation of neighbouring Digit 3 cortical sites, possibly as a result of disinhibition. This later interpretation is supported by tactile discrimination results showing that subjects with carpal tunnel syndrome had significantly slower response times and larger error rates for detecting stimulation of median nerve-innervated digits than did healthy controls.

Finally, we evaluated the source time courses in contralateral S2. Previous functional MRI work has suggested that responses within both S1 and S2 are altered in chronic pain populations (Pleger et al., 2006). In the current study, contralateral S2 response in subjects with carpal tunnel syndrome was largest for Digit 5 at long latencies. This was not the case in healthy control subjects. Furthermore, no significant differences in response magnitude were found between healthy controls and subjects with carpal tunnel syndrome. The lack of consistent contralateral S2 differences between groups suggests that response in this area may not be a strong marker of maladaptive plasticity in carpal tunnel syndrome. However, another possibility is that the interstimulus interval ($<2.0\,s$) used in our study was too short to investigate differences in S2 MEG response between groups. It is also possible that paradigms specifically exploiting long latency electrophysiological responses, such as a pain task, would be more useful to reveal differences in S2 event-related fields between carpal tunnel syndrome and healthy controls.

Decreased Beta event-related desynchronization correlates with paraesthesia intensity

It is well known that somatosensory stimulation modulates oscillatory activity within contralateral sensorimotor cortex (Pfurtscheller, 1981; Salmelin and Hari, 1994). Specifically, brief, innocuous tactile stimulation produces event-related desynchronization in the alpha (~ 7–$14\,Hz$) and beta (15–$30\,Hz$) frequency ranges at ~ 100–$400\,ms$ post-stimulus (Nikouline et al., 2000; Cheyne et al., 2003). When the interstimulus interval is sufficiently long, this event-related desynchronization is followed by a beta band event-related synchronization at $>400\,ms$, often referred to as the beta 'rebound' (Salenius et al., 1997). Furthermore, sensorimotor beta increases when subjects are given GABA agonists (Jensen et al., 2005), suggesting that these rhythms are at least, in part, under inhibitory GABAergic control.

We found that for stimulation of median nerve-innervated digits, post-stimulus beta event-related desynchronization at ~ 200–$320\,ms$ was significantly weaker in subjects with carpal tunnel syndrome than in healthy controls (Fig. 3). Beta event-related desynchronization was also weaker for Digits 2 and 3 compared with Digit 5 in subjects with carpal tunnel syndrome at ~ 150–$200\,ms$. In the current study, altered beta event-related desynchronization was not due to differences in stimulus level, as this did not vary significantly across subjects. Furthermore, beta event-related desynchronization has been shown to have little dependence on fine gradations in stimulus intensity (Stancak et al., 2003). Interestingly, subjects with

stronger symptoms of paraesthesias also had less post-stimulus beta event-related desynchronization (Fig. 6B). These changes in beta event-related desynchronization were not correlated with nerve conduction velocity. Thus, long latency modification in brain responses (i.e. after cessation of the event-related field) is likely to represent more complex intracortical processing.

Furthermore, we found that the beta event-related synchronization or 'rebound' began earlier in subjects with carpal tunnel syndrome. In addition to altered somatotopy (Pleger et al., 2004), previous studies have found that the extent (duration and magnitude) of the rebound in response to innocuous stimulation may be altered in chronic pain states (Juottonen et al., 2002). For example, decreased beta event-related synchronization to noxious stimulation in complex regional pain syndrome has been postulated to reflect attenuated motor reactivity (Kirveskari et al., 2010). Although Kirveskari et al. (2010) also showed that beta event-related desynchronization was slightly diminished (albeit non-significantly), a significantly diminished rebound was interpreted as disinhibition of motor cortex caused by the existing pain state. Thus, complex regional pain syndrome may involve static hyperexcitation, whereby external noxious stimulation will not further activate motor areas because of a ceiling effect. With regard to the current carpal tunnel syndrome data, it is possible that random spontaneous afference, in the form of continuous paraesthesias, renders the underlying median nerve innervated cortex 'busy'. This would result in an overall decrease in neuronal resources available for processing applied somatosensory stimuli as exemplified by decreased event-related desynchronization in response to median nerve-innervated digit stimulation.

Digit separation distance is smaller in carpal tunnel syndrome

Cortical remapping as a result of altered afferent signalling has been demonstrated after peripheral nerve lesions in animals (Merzenich et al., 1983a, 1984; Calford and Tweedale, 1991; Pons et al., 1991), limb amputation in humans (Ramachandran et al., 1992; Elbert et al., 1994; Knecht et al., 1995; Flor, 2003), spinal injury (Moore et al., 2000), temporary finger webbing (Stavrinou et al., 2007) and even anaesthetic block of afferent sensory information (Rossini et al., 1994). Importantly, persistent pain and/or paraesthesias resulting from deafferentation can induce long-lasting modifications at the spinal, subcortical and cortical level (Knecht et al., 1995; Davis et al., 1996; Birbaumer et al., 1997; Tinazzi et al., 1998, 2004; Costigan et al., 2009).

Neuroimaging data from MEG (Tecchio et al., 2002) and functional MRI (Napadow et al., 2006) suggest that pain and/or paraesthesias caused by median nerve compression may result in altered cortical digit separation distance. Here, we found that separation distances between Digits 2 and 3 were significantly smaller for subjects with carpal tunnel syndrome compared with healthy controls. Interestingly, previous work showed that carpal tunnel syndrome patients with predominant pain symptoms had decreased Digit 1–Digit 5 digit separation, whereas those with predominant paraesthesias demonstrated the opposite (Tecchio et al., 2002). Although we did not evaluate the cortical

representation of Digit 1, our patient sample had paraesthesias predominate over pain. Thus, although patients with carpal tunnel syndrome did not differ significantly in Digit 2–Digit 5 separation distance compared with healthy adults, it is possible that Digit 1–Digit 5 separation was greater in our sample. Furthermore, our finding of decreased Digit 2–Digit 3 separation is similar to Napadow et al. (2006) who reported that less distinct or 'blurred' representations for median nerve-innervated digits results from prolonged, diffuse, multi-digit paraesthesias and Hebbian neuroplasticity. For example, paraesthesias in Digits 1–4 may reflect greater temporal coherence of signalling between these digits than is normally experienced. Thus, with respect to classical Hebbian plasticity (Hebb, 1949), increased temporal synchrony may produce synaptic strengthening and cortical reorganization that appears as a blurring of median nerve-innervated digit representations in carpal tunnel syndrome. Previous data have shown that synchronous multi-digit co-activation can produce blurred cortical representations in animals (Wang et al., 1995; Godde et al., 1996) and humans (Pilz et al., 2004). Similarly, surgically induced syndactyly also produces overlap of S1 cortical representation fields for fused digits (Clark et al., 1988; Allard et al., 1991).

Conclusion

To our knowledge, the present results are the first to demonstrate significant changes in the temporal dynamics of cortical-evoked response and induced oscillatory activity in carpal tunnel syndrome. Specifically, S1 M20 latencies for median nerve-innervated digits were longer in carpal tunnel syndrome; thus, slower peripheral nerve conduction velocity corresponds to greater delays in the latency of the first cortical response. Larger M30/M20 ratios in carpal tunnel syndrome may indicate co-activation of neighbouring median nerve-innervated digits related to cortical GABAergic disinhibition. This interpretation is supported by tactile discrimination results showing that subjects with carpal tunnel syndrome had significantly slower response times and larger error rates for detecting stimulation of median nerve-innervated digits than healthy controls. Furthermore, subjects with carpal tunnel syndrome demonstrated weaker post-stimulus beta event-related desynchronization and earlier and shorter event-related synchronization, the former being correlated with increasing paraesthesia ratings. One explanation is that spontaneous irregular afferent signalling in median nerve-innervated digits, i.e. paraesthesias, renders their corresponding sensorimotor areas 'busy' to externally applied stimuli. Finally, S1 digit somatotopy demonstrated the presence of 'blurring' of median nerve-innervated digit representations, which may be due to ongoing paraesthesias and Hebbian plasticity.

In conclusion, this study reveals significant correlation between the clinical severity of carpal tunnel syndrome and the latency of the early M20, as well as the strength of long latency beta oscillations. These temporal MEG measures are novel markers of neuroplasticity in carpal tunnel syndrome and could be used to study central changes that may occur following clinical intervention.

Acknowledgements

Funding

References

Allard T, Clark SA, Jenkins WM, Merzenich MM. Reorganization of somatosensory area 3b representations in adult owl monkeys after digital syndactyly. J Neurophysiol 1991; 66: 1048–58.

Birbaumer N, Lutzenberger W, Montoya P, Larbig W, Unertl K, Topfner S, et al. Effects of regional anesthesia on phantom limb pain are mirrored in changes in cortical reorganization. J Neurosci 1997; 17: 5503–8.

Calford MB, Tweedale R. Immediate expansion of receptive fields of neurons in area 3b of macaque monkeys after digit denervation. Somatosens Mot Res 1991; 8: 249–60.

Cheyne D, Gaetz W, Garnero L, Lachaux JP, Ducorps A, Schwartz D, et al. Neuromagnetic imaging of cortical oscillations accompanying tactile stimulation. Brain Res Cogn Brain Res 2003; 17: 599–611.

Clark SA, Allard T, Jenkins WM, Merzenich MM. Receptive fields in the body-surface map in adult cortex defined by temporally correlated inputs. Nature 1988; 332: 444–5.

Costigan M, Scholz J, Woolf CJ. Neuropathic pain: a maladaptive response of the nervous system to damage. Annu Rev Neurosci 2009; 32: 1–32.

Dale AM, Fischl B, Sereno MI. Cortical surface-based analysis. I. Segmentation and surface reconstruction. Neuroimage 1999; 9: 179–94.

Dale AM, Halgren E. Spatiotemporal mapping of brain activity by integration of multiple imaging modalities. Curr Opin Neurobiol 2001; 11: 202–8.

Dale AM, Liu AK, Fischl BR, Buckner RL, Belliveau JW, Lewine JD, et al. Dynamic statistical parametric mapping: combining fMRI and MEG for high-resolution imaging of cortical activity. Neuron 2000; 26: 55–67.

Dale AM, Sereno MI. Improved localization of cortical activity by combining EEG and MEG with MRI cortical surface reconstruction: a linear approach. J Cogn Neurosci 1993; 5: 162–76.

Davis KD, Kiss ZH, Tasker RR, Dostrovsky JO. Thalamic stimulation-evoked sensations in chronic pain patients and in nonpain (movement disorder) patients. J Neurophysiol 1996; 75: 1026–37.

deMunck JC. A linear dicretization of the volume conductor boundary integral equation using analytically integrated elements. IEEE Transact Biomed Eng 1992; 39: 986–90.

Dhond RP, Buckner RL, Dale AM, Marinkovic K, Halgren E. Spatiotemporal maps of brain activity underlying word generation and their modification during repetition priming. J Neurosci 2001; 21: 3564–71.

Druschky K, Kaltenhauser M, Hummel C, Druschky A, Huk WJ, Stefan H, et al. Alteration of the somatosensory cortical map in peripheral mononeuropathy due to carpal tunnel syndrome. Neurorep 2000; 11: 3925–30.

Elbert T, Flor H, Birbaumer N, Knecht S, Hampson S, Larbig W, et al. Extensive reorganization of the somatosensory cortex in adult humans after nervous system injury. Neuroreport 1994; 5: 2593–7.

Fischl B, Sereno MI, Dale AM. Cortical surface-based analysis. II. Inflation, flattening, and a surface-based coordinate system. Neuroimage 1999a; 9: 195–207.

Fischl B, Sereno MI, Tootell RB, Dale AM. High-resolution intersubject averaging and a coordinate system for the cortical surface. Hum Brain Mapp 1999b; 8: 272–84.

Flor H. Remapping somatosensory cortex after injury. Adv Neurol 2003; 93: 195–204.

Forss N, Merlet I, Vanni S, Hamalainen M, Mauguiere F, Hari R. Activation of human mesial cortex during somatosensory target detection task. Brain Res 1996; 734: 229–35.

Godde B, Spengler F, Dinse HR. Associative pairing of tactile stimulation induces somatosensory cortical reorganization in rats and humans. Neuroreport 1996; 8: 281–5.

Goupillaud P, Grossman A, Morlet J. Cycle-octave and related transforms in seismic signal analysis. Geoexploration 1984; 23: 85–102.

Graimann B, Huggins JE, Levine SP, Pfurtscheller G. Visualization of significant ERD/ERS patterns in multichannel EEG and ECoG data. Clin Neurophysiol 2002; 113: 43–7.

Hakim AJ, Cherkas L, El Zayat S, MacGregor AJ, Spector TD. The genetic contribution to carpal tunnel syndrome in women: a twin study. Arthritis Rheum 2002; 47: 275–9.

Halgren E, Dhond RP, Christensen N, Van Petten C, Marinkovic K, Lewine JD, et al. N400-like magnetoencephalography responses modulated by semantic context, word frequency, and lexical class in sentences. Neuroimage 2002; 17: 1101–16.

Hamalainen MS, Ilmoniemi RJ. Interpreting measured magnetic fields of the brain: estimates of current distribution. Helsinki: University of Technology, Department of Technical Physics, Report TKK-F-A559; 1984.

Hebb D. The organization of behavior. New York: Wiley and Sons; 1949.

Jablecki CK, Andary MT, Floeter MK, Miller RG, Quartly CA, Vennix MJ, Wilson JR. Practice parameter: Electrodiagnostic studies in carpal tunnel syndrome. Report of the American Association of Electrodiagnostic Medicine, American Academy of Neurology, and the American Academy of Physical Medicine and Rehabilitation. Neurology 2002; 58: 1589–92.

Jensen O, Goel P, Kopell N, Pohja M, Hari R, Ermentrout B. On the human sensorimotor-cortex beta rhythm: sources and modeling. Neuroimage 2005; 26: 347–55.

Juottonen K, Gockel M, Silen T, Hurri H, Hari R, Forss N. Altered central sensorimotor processing in patients with complex regional pain syndrome. Pain 2002; 98: 315–23.

Katz JN, Keller RB, Simmons BP, Rogers WD, Bessette L, Fossel AH, et al. Maine Carpal Tunnel Study: outcomes of operative and nonoperative therapy for carpal tunnel syndrome in a community-based cohort. J Hand Surg Am 1998; 23: 697–710.

Katz JN, Simmons BP. Clinical practice. Carpal tunnel syndrome. N Engl J Med 2002; 346: 1807–12.

Kirveskari E, Vartiainen NV, Gockel M, Forss N. Motor cortex dysfunction in complex regional pain syndrome. Clin Neurophysiol 2010; 121: 1085–91.

Knecht S, Henningsen H, Elbert T, Flor H, Hohling C, Pantev C, et al. Cortical reorganization in human amputees and mislocalization of painful stimuli to the phantom limb. Neurosci Lett 1995; 201: 262–4.

Levine DW, Simmons BP, Koris MJ, Daltroy LH, Hohl GG, Fossel AH, et al. A self-administered questionnaire for the assessment of severity of symptoms and functional status in carpal tunnel syndrome. J Bone Joint Surg Am 1993; 75: 1585–92.

Lin FH, Belliveau JW, Dale AM, Hamalainen MS. Distributed current estimates using cortical orientation constraints. Hum Brain Mapp 2006; 27: 1–13.

Liu AK, Belliveau JW, Dale AM. Spatiotemporal imaging of human brain activity using fMRI constrained MEG data: Monte Carlo simulations. Proc Natl Acad Sci USA 1998; 95: 8945–50.

Marinkovic K. Spatiotemporal dynamics of word processing in the human cortex. Neuroscientist 2004; 10: 142–52.

Mauguiere F, Merlet I, Forss N, Vanni S, Jousmaki V, Adeleine P, et al. Activation of a distributed somatosensory cortical network in the human brain. A dipole modelling study of magnetic fields evoked by median nerve stimulation. Part I: location and activation timing of SEF sources. Electroencephalogr Clin Neurophysiol 1997a; 104: 281–9.

Mauguiere F, Merlet I, Forss N, Vanni S, Jousmaki V, Adeleine P, et al. Activation of a distributed somatosensory cortical network in the human brain: A dipole modelling study of magnetic fields evoked by median nerve stimulation. Part II: Effects of stimulus rate, attention and stimulus detection. Electroencephalogr Clin Neurophysiol 1997b; 104: 290–5.

Mendez P, Bacci A. Assortment of GABAergic plasticity in the cortical interneuron melting pot. Neural Plast 2011; 2011: 976856.

Merzenich MM, Kaas JH, Wall J, Nelson RJ, Sur M, Felleman D. Topographic reorganization of somatosensory cortical areas 3b and 1 in adult monkeys following restricted deafferentation. Neuroscience 1983a; 8: 33–55.

Merzenich MM, Kaas JH, Wall JT, Sur M, Nelson RJ, Felleman DJ. Progression of change following median nerve section in the cortical representation of the hand in areas 3b and 1 in adult owl and squirrel monkeys. Neuroscience 1983b; 10: 639–65.

Merzenich MM, Nelson RJ, Stryker MP, Cynader MS, Schoppmann A, Zook JM. Somatosensory cortical map changes following digit amputation in adult monkeys. J Comp Neurol 1984; 224: 591–605.

Moore CI, Stern CE, Dunbar C, Kostyk SK, Gehi A, Corkin S. Referred phantom sensations and cortical reorganization after spinal cord injury in humans. Proc Natl Acad Sci USA 2000; 97: 14703–8.

Napadow V, Kettner N, Ryan A, Kwong KK, Audette J, Hui KK. Somatosensory cortical plasticity in carpal tunnel syndrome–a cross-sectional fMRI evaluation. Neuroimage 2006; 31: 520–30.

Nikouline VV, Linkenkaer-Hansen K, Wikstrom H, Kesaniemi M, Antonova EV, Ilmoniemi RJ, et al. Dynamics of mu-rhythm suppression caused by median nerve stimulation: a magnetoencephalographic study in human subjects. Neurosci Lett 2000; 294: 163–6.

Oldfield RC. The assessment and analysis of handedness: the Edinburgh inventory. Neuropsychologia 1971; 9: 97–113.

Oostendorp TF, Van Oosterom A. Source parameter estimation using realistic geometry in bioelectricity and biomagnetism. In: Nenonen J, Rajala HM, Katila T, editors. Biomagnetic localization and 3D modeling. Helsinki. Helsinki University of Technology, Report TKK-F-A689, 1992.

Office of Women's Health. Carpal tunnel syndrome fact sheet. In: U.S. Department of Health and Human Services, editor; 2009. p. 1–5.

Penfield W, Rasmussen T. The cerebral cortex of man. New York: Macmillan; 1955.

Pfurtscheller G. Central beta rhythm during sensorimotor activities in man. Electroencephalogr Clin Neurophysiol 1981; 51: 253–64.

Phalen GS. The carpal-tunnel syndrome. Seventeen years' experience in diagnosis and treatment of six hundred fifty-four hands. J Bone Joint Surg Am 1966; 48: 211–28.

Pilz K, Veit R, Braun C, Godde B. Effects of co-activation on cortical organization and discrimination performance. Neuroreport 2004; 15: 2669–72.

Pleger B, Ragert P, Schwenkreis P, Forster AF, Wilimzig C, Dinse H, et al. Patterns of cortical reorganization parallel impaired tactile discrimination and pain intensity in complex regional pain syndrome. Neuroimage 2006; 32: 503–10.

Pleger B, Tegenthoff M, Schwenkreis P, Janssen F, Ragert P, Dinse HR, et al. Mean sustained pain levels are linked to hemispherical side-to-side differences of primary somatosensory cortex in the complex regional pain syndrome I. Exp Brain Res 2004; 155: 115–9.

Pons TP, Garraghty PE, Ommaya AK, Kaas JH, Taub E, Mishkin M. Massive cortical reorganization after sensory deafferentation in adult macaques. Science 1991; 252: 1857–60.

Porcaro C, Coppola G, Di Lorenzo G, Zappasodi F, Siracusano A, Pierelli F, et al. Hand somatosensory subcortical and cortical sources assessed by functional source separation: an EEG study. Hum Brain Mapp 2009; 30: 660–74.

Radwin RG, Sesto ME, Zachary SV. Functional tests to quantify recovery following carpal tunnel release. J Bone Joint Surg Am 2004; 86A: 2614–20.

Ramachandran VS, Stewart M, Rogers-Ramachandran DC. Perceptual correlates of massive cortical reorganization. Neuroreport 1992; 3: 583–6.

Rossini PM, Martino G, Narici L, Pasquarelli A, Peresson M, Pizzella V, et al. Short-term brain 'plasticity' in humans: transient finger representation changes in sensory cortex somatotopy following ischemic anesthesia. Brain Res 1994; 642: 169–77.

Salenius S, Schnitzler A, Salmelin R, Jousmaki V, Hari R. Modulation of human cortical rolandic rhythms during natural sensorimotor tasks. Neuroimage 1997; 5: 221–8.

Salmelin R, Hari R. Spatiotemporal characteristics of sensorimotor neuromagnetic rhythms related to thumb movement. Neuroscience 1994; 60: 537–50.

Seiler JG 3rd, Milek MA, Carpenter GK, Swiontkowski MF. Intraoperative assessment of median nerve blood flow during carpal tunnel release with laser Doppler flowmetry. J Hand Surg Am 1989; 14: 986–91.

Seung HS. How the brain keeps the eyes still. Proc Natl Acad Sci USA 1996; 93: 13339–44.

Silverstein BA, Fine LJ, Armstrong TJ. Occupational factors and carpal tunnel syndrome. Am J Ind Med 1987; 11: 343–58.

Stancak A, Svoboda J, Rachmanova R, Vrana J, Kralik J, Tintera J. Desynchronization of cortical rhythms following cutaneous stimulation: effects of stimulus repetition and intensity, and of the size of corpus callosum. Clin Neurophysiol 2003; 114: 1936–47.

Stavrinou ML, Della Penna S, Pizzella V, Torquati K, Cianflone F, Franciotti R, et al. Temporal dynamics of plastic changes in human primary somatosensory cortex after finger webbing. Cereb Cortex 2007; 17: 2134–42.

Tecchio F, Padua L, Aprile I, Rossini PM. Carpal tunnel syndrome modifies sensory hand cortical somatotopy: a MEG study. Hum Brain Mapp 2002; 17: 28–36.

Tiihonen J, Hari R, Hamalainen M. Early deflections of cerebral magnetic responses to median nerve stimulation. Electroencephalogr Clin Neurophysiol 1989; 74: 290–6.

Tinazzi M, Valeriani M, Moretto G, Rosso T, Nicolato A, Fiaschi A, et al. Plastic interactions between hand and face cortical representations in patients with trigeminal neuralgia: a somatosensory-evoked potentials study. Neuroscience 2004; 127: 769–76.

Tinazzi M, Zanette G, Volpato D, Testoni R, Bonato C, Manganotti P, et al. Neurophysiological evidence of neuroplasticity at multiple levels of the somatosensory system in patients with carpal tunnel syndrome. Brain 1998; 121(Pt 9): 1785–94.

Tinel J. "Tingling" signs with peripheral nerve injuries. 1915. J Hand Surg Br 2005; 30: 87–9.

Wang X, Merzenich MM, Sameshima K, Jenkins WM. Remodelling of hand representation in adult cortex determined by timing of tactile stimulation. Nature 1995; 378: 71–5.

Wikstrom H, Huttunen J, Korvenoja A, Virtanen J, Salonen O, Aronen H, et al. Effects of interstimulus interval on somatosensory evoked magnetic fields (SEFs): a hypothesis concerning SEF generation at the primary sensorimotor cortex. Electroencephalogr Clin Neurophysiol 1996; 100: 479–87.

Zhang Z, Francisco EM, Holden JK, Dennis RG, Tommerdahl M. Somatosensory information processing in the aging population. Front Aging Neurosci 2011; 3: 18.